Journal of Alloys and Compounds 509 (2011) 5600–5603

Contents lists available at ScienceDirect

Journal of Alloys and Compounds

journal homepage: www.elsevier.com/locate/jallcom

Magnetic multiresonance behavior of Fe@Al_2O_3 nanoembedments and microstructural evolution during mechanosynthesis

Zhi-cheng Shi[a], Zi-dong Zhang[a], Jing-yan Guo[a], Meng Gao[a], Xiao-gang Qi[a], Jian-qiang Bi[a], Run-hua Fan[a,*], Wei-hsing Tuan[b]

[a] Key Laboratory for Liquid-Solid Structural Evolution and Processing of Materials (Ministry of Education), Shandong University, Jinan 250061, China
[b] Department of Materials Science and Engineering, Taiwan University, Taipei 106, Taiwan

ARTICLE INFO

Article history:
Received 8 October 2010
Received in revised form 16 February 2011
Accepted 17 February 2011
Available online 23 February 2011

Keywords:
Milling
Nanocomposites
Magnetic properties
Al_2O_3
Microwave properties

ABSTRACT

The embedding of metal nanoparticles into an insulating ceramic matrix can provide encapsulation and prevent their oxidation and agglomeration. A nanoembedment powder with the Fe nanoparticles embedded into Al_2O_3 matrix is prepared by high-energy ball milling. Starting from the highly exothermic reactant mixture of magnetite and aluminum, Fe nanoparticles were in situ formed in Al_2O_3 matrix by mechanochemical reaction. It is found that a post-reaction milling significantly narrows the size distribution of Fe nanoparticles. The mechanism for the two-stage milling process was proposed. The microwave permeability of nanoembedments exhibited a multiresonance behavior, which was the evidence for monodispersed Fe nanoparticles. The Fe@Al_2O_3 nanoembedments are potential candidates as microwave absorber and left-handed materials.

1. Introduction

The nanoembedments refer to some nanocomposites with metal nanoparticles, such as Fe, Ni or Co, embedded in an insulating ceramic matrix. The insulating embedment can provide encapsulation and prevent oxidation and agglomeration of metal nanoparticles.

Nanoembedments are of significant technological importance in many applications, such as bioapplications [1], catalytic reactions [2], and electromagnetic applications [3,4]. In particular, magnetic nanoembedments consisting of magnetic nanoparticles encapsulated by insulating hosts have attracted considerable attention owing to their wide range of applications, such as magnetic resonance imaging (MRI) [5], magnetic fluid [6], novel high frequency soft magnetic materials [7,8] and magnetic drug carriers [9]. Physical properties of such nanoembedments are influenced by their size, size distribution and volume fraction of the metal nanoparticles. Therefore, in order to fully realize their technological application, the microstructure control is a significant issue.

These nanocomposite powders have been prepared by directly milling of metal and ceramic powders [10,11], or by chemical methods involving the reduction in hydrogen of suitable oxide precursors [12]. The mechanosynthesis, or named as mechanochemical synthesis, has been attracting increasing interest in relation to the extensions of solid solubility [13], disordering of intermetallics, solid-state amorphization [14]. The most significant characteristic of this process is that the synthesis of the designed materials is activated by mechanical energy, instead of the thermal energy required in the conventional solid-state reaction process. This technique has the advantages over both the conventional solid-state reaction and the wet-chemistry-based processing routes for several reasons. First, it uses cost-effective and widely available oxides as the starting materials. Second, it takes place at room temperature, thus effectively produces unique microstructure. The mechanosynthesis has been considered as one of the best ways to fabricate nanoembedments powders with highly controlled microstructure. This method is effective in making a nanoembedment with fine and well-dispersed metal nanoparticles and strong bonding to ceramic matrix. The morphology of the metal nanoparticles could be controlled by altering the composition and milling conditions. As a branch of chemistry concerning with room-temperature solid state reaction which is induced by mechanical energy, mechanochemical synthesis has been successfully employed to synthesize a wide range of nanocrystalline ceramic powders. Bobić et al. successfully prepared $BaBi_4Ti_4O_{15}$ ferroelectric ceramic using non-conventional solid-state reaction route based on mechanochemical synthesis during intensive milling [15]. Moreover, Ni–Zn and Mn–Zn ferrite nanoparticles were also synthesized via mechanochemical route by Amiri et al. [16]. Cristóbal et al. obtained polycrystalline $Y_{0.5}La_{0.5}FeO_3$ orthofer-

* Corresponding author. Tel.: +86 531 88393396; fax: +86 531 88395011.
E-mail address: fan@sdu.edu.cn (R.-h. Fan).

0925-8388/$ – see front matter © 2011 Elsevier B.V. All rights reserved.
doi:10.1016/j.jallcom.2011.02.082

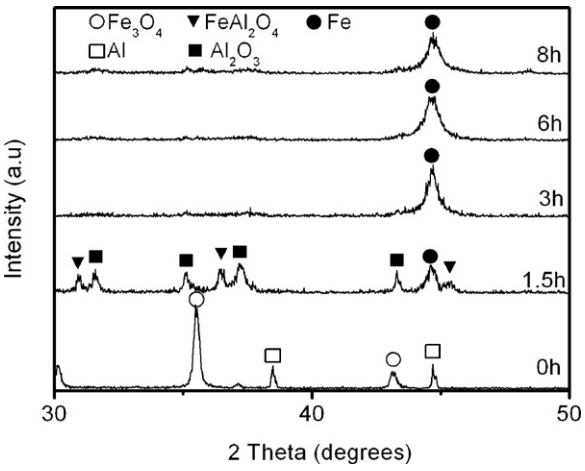

Fig. 1. XRD patterns of Al-Fe_3O_4 before and after various ball milling times.

rite powder by mechanochemical activation of Fe_3O_4–La_2O_3–Y_2O_3 reactive mixtures [17]. Furthermore, mechanosynthesis was also employed to prepare various nanocomposites. Sabooni et al. successfully synthesized Cu(Mo)/30 vol.% α-Al_2O_3 nanocomposite by a displacement reaction between Al and MoO_3 in ball milling of initial Cu, MoO_3 and Al powders [18]. Sun et al. successfully synthesized Mo–Cu nanocomposite powders by the mechanochemical and hydrogen-reduction process [19].

Although a remarkable progress has been made in the preparation of nanoembedments by using mechanosynthesis over the past few years [20], the microstructural evolution during mechanical milling still requires a profound investigation. This study attempts to correlate the physical properties of Fe@Al_2O_3 nanoembedments with its structural characteristic, e.g. the size and its distribution of iron nanoparticles.

2. Experimental procedures

The magnetite powder (purity ≥ 99.0%, 2–4 μm) and aluminum powder (purity ≥ 99.0%, 200 meshes) were mixed in a molar ratio of 3:8. In the final product, the expected Fe content is 55.3 wt.% or 38.2 vol.%. The mixtures were milled up to 8 h using a planetary mill and a stainless vial with hardened Cr balls of 8 mm in diameter under argon atmosphere. The weight ratio of balls to powder is 40:1. The phase composition was analyzed by an X-ray diffractometer (D/max-2400, Rigaku Corp., Tokyo, Japan) with Cu Kα radiation. The microstructure of milled products was examined by scanning electron microscope (SEM, JSM-6380LA, Joel Co., Japan) and transmission electron microscope (TEM, H-800, Hitachi Co., Japan). The static magnetic properties were measured at room temperature by vibrating sample magnetometer (VSM, 7410, Lake Shore Co., USA). The microwave properties were measured with a vector network analyzer (VNA, 8753ES, Agilent Co., USA) in the frequency range of 2–18 GHz. The samples for microwave measurement were prepared by mixing powders (75 wt.%) and paraffin wax, and molding in a coaxial die with 7 mm in outer diameter and 3 mm in inner diameter.

3. Results and discussion

The XRD patterns of the Al-Fe_3O_4 powder mixture before and after various milling times are shown in Fig. 1. After 1.5 h milling, the mechanical activation induces a self-sustained reaction, which results in the formation of α-Fe and α-Al_2O_3, along with the hercynite ($FeAl_2O_4$). Mössbauer spectra for the mechanochemical products of Al-Fe_3O_4 mixture carried out by Botta et al. indicated that about 70% iron element exists in the form of α-Fe while the remaining in $FeAl_2O_4$ [21]. After 3 h milling, the starting materials and the intermediate phase of hercynite have been almost completely consumed. No Al_2O_3 peak is detected, indicating that the structure of the alumina matrix is amorphous. With extensive milling up to 8 h, no apparent changes can be observed in the XRD patterns. Generally speaking, the introduction of contamination in ball milling is inevitable, and the level of contamination increases if the powder is milled for long time [14]. In the conventional preparation procedure of Fe/Al_2O_3 nanocomposites, long milling time up to 70 h is necessary for Fe-Al_2O_3 powder mixture [10]. However, in our present work, mechanochemical technique was used to prepare Fe/Al_2O_3 nanoembedments and the milling time was greatly shortened to 3 h, leading to less contamination. Fig. 2 shows the morphology of powders milled after 3 and 6 h, respectively. While the SEM image (Fig. 2a) indicates the powder size of around several micrometers for 3 h products, the TEM image (Fig. 2b) shows that the Fe nanoparticles are smaller than 30 nm. These results suggest that Fe nanoparticles have been successfully embedded into alumina matrix after 3 h milling. Extensively milling up to 6 h seems to narrow the size distribution of Fe particles around 25 nm, consequently increases the average particle size, as shown in Fig. 2c. In order to understand the relationship between the microstructure and the magnetic properties of Fe@Al_2O_3, the hysteresis loops of the milled powders were determined as a function of milling time. Fig. 3 shows the milling time dependence of the saturation magnetization (M_s) and coercivity (H_c). It is observed that magnetization has less variation after 3 h milling, indicating that the fraction of α-Fe remains almost the same during extensive milling. However, the coercivity increases monotonously with the milling time, attaining the value of 125 Oe after 8 h milling. This is in agreement with the trend reported by Löffler et al. [22]. For the very fine Fe nanoparticles of several nanometers, H_c remains zero due to superparamagnetic effect, and then H_c increases with increasing the size of Fe particles.

The authors proposed a two-stage model for the synthesis of monodispersed Fe@Al_2O_3 nanoembedments. For the starting mixture of Al-Fe_3O_4 used in the present work, the mechanical milling may lead to the following reaction:

$$8Al + 3Fe_3O_4 \rightarrow 4Al_2O_3 + 9Fe \quad (1)$$

The reaction is a highly exothermic one (ΔH = 3021 kJ/mol). Al-Fe_3O_4 mixture belongs to ductile–brittle system. In the first stage of milling, while the brittle magnetite powders are mainly fractured, ductile Al powders are repeatedly flattened, cold welded, fractured and rewelded. These fragmented brittle powders tend to become included in the ductile powders. The mechanical milling increases the area of contact between the reactant powders due to a reduction in particle size and allows fresh surfaces to come into contact repeatedly [14]. At the initial stage of mechanical milling, reaction (1) has taken place in localized regions. However, the energy provided by the mechanical treatment and that released by the local reaction are not enough to overcome the energy lost through heat dissipation. So reaction (1) is not fully initiated. The products of reaction (1), Fe and Al_2O_3, partially react with the remaining magnetite, resulting in the formation of hercynite. And then the intermediate hercynite reacts with Al to form the final Fe and Al_2O_3 [21]. After the combustion reaction is completed, the second stage of milling concerns a newly formed ductile–brittle system: chemically stable Fe-Al_2O_3 nanocomposites, instead of the initial Al-Fe_3O_4 microscaled mixture. While the alumina remains amorphous, the size of Fe nanoparticles increases with increasing milling time, rather than the refinement commonly observed in mechanical milling. This phenomenon could be explained by milling mechanism. During mechanical attrition, the underlying refinement mechanism is governed by plastic deformation via dislocation motion. However, the ultrafine iron nanoparticles synthesized by the mechanosynthesis are dislocation free, the very high stresses required for dislocation movement hinder the plastic deformation of the nanoparticles. Hence, further refinement by milling seems to be impossible, further milling can only be accomplished by grain boundary sliding, which results in the monodispersed Fe@Al_2O_3 by slightly increasing of the size of Fe nanoparticles. When the milling

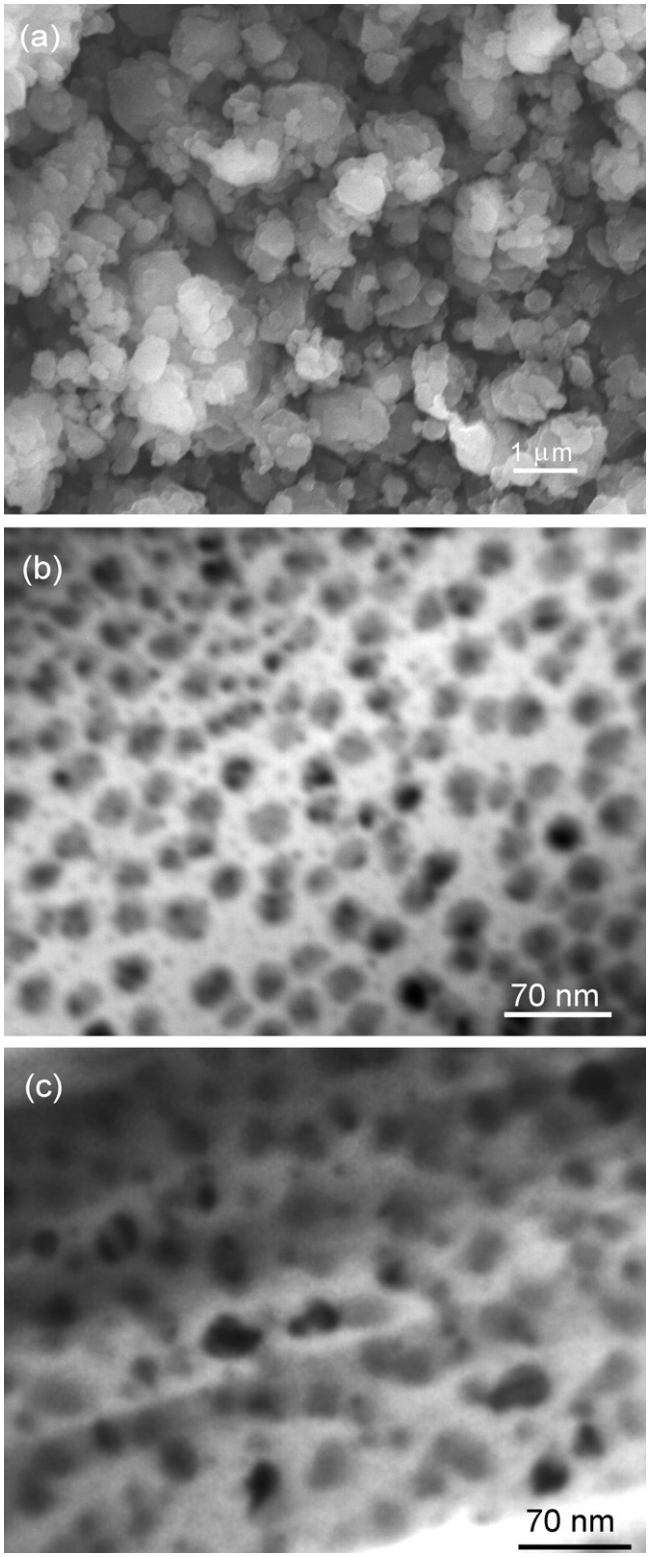

Fig. 2. SEM (a) and TEM (b and c) images of a Fe@Al_2O_3 nanoembedment powder: (a and b) 3 h milled, c) 6 h milled.

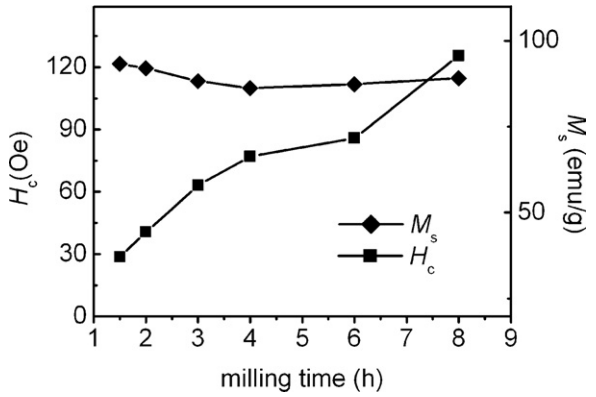

Fig. 3. Dependence of the saturation magnetization and coercivity of milled products on milling time.

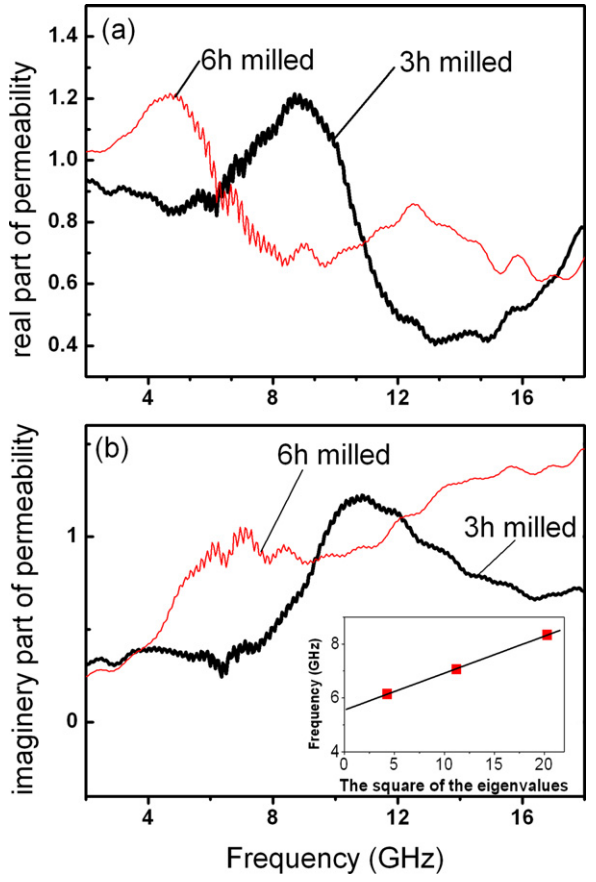

Fig. 4. Real (a) and imaginary (b) part of permeability of 3 h and 6 h milled powders. The inset shows the plot of the resonance frequency versus the square of the eigenvalues μ_{kn} for 6 h milled powders.

extends from 3 h to 6 h, the only characteristic of iron nanoparticles which varies is the size and its distribution.

Microwave properties are sensitive to the microstructure, especially to the size and size distribution of Fe nanoparticles. Fig. 4 shows a relaxation-type frequency dispersion of permeability for the nanoembedment powders mixed with paraffin wax. The curves exhibit a broadened resonance band, which is shifted to lower frequency for the 6 h milled sample. The shifts may be considered as a size effect. Since extensive milling after mechanochemical reaction can change the size of iron nanoparticles, we are able to follow the effect of this change from the permeability curves. According to the natural resonance equation [23]:

$$2\pi f_r = \gamma H_a \quad (2)$$

where γ is the gyromagnetic ratio, H_a the anisotropic fields. The resonance frequency f_r may be reduced when the anisotropic field decreases for larger Fe nanoparticles [24]. For electromagnetic

wave absorption materials applied in different microwave range, it is beneficial to tune the resonance frequency through the control on the size of magnetic nanoparticles. Fig. 4b also shows the splitting of resonance band into three peaks for the 6 h milled sample. Such a multiresonance behavior was reported also with Fe–Co–Ni nanoparticles by Viau et al. [25]. This behavior is correlated to the size effect of ferromagnetic particles. It was pointed out that particles size below the order of ~100 nm and a narrow distribution of particle size are necessary for observing multiresonance [25]. This size effect can be qualitatively related to exchange resonance modes proposed by Aharoni [26]. The resonance frequencies ω are given by [26].

$$\frac{\omega}{\gamma_0} = \frac{C\mu_{kn}^2}{R^2 M_S} + H_0 - \frac{4\pi}{3}M_S + \frac{2K_1}{M_S} \quad (3)$$

where γ_0 is the gyromagnetic ratio, $C = 2A$ the exchange constant, μ_{kn} the eigenvalues of the equation $[J_n'(r)]_{r=R} = 0$ with J_n being spherical Bessel functions, R the particle radius, M_s the saturation magnetization, H_0 the external magnetic field, and K_1 the magnetocrystalline anisotropy constant. The values of the resonance frequencies were plotted versus the squares of eigenvalues μ_{kn} ($\mu_{11} = 2.08$, $\mu_{12} = 3.34$, $\mu_{13} = 4.51$ [25]), as shown in the inset to Fig. 4b. A linear relationship is observed. By knowing the $R = 12.5 \times 10^{-9}$ m and $M_s = 1700$ kA/m, an experimental value (1.5×10^{-12} J m^{-1}) of the exchange constant A can be obtained from the slope of the straight line. Similar to that of Fe clusters embedded in Ag [27], A is lower than 10^{-11} J m^{-1}, the values reported for bulk Fe. It indicates a low exchange interaction for nanostructured ferromagnets [22].

Theoretically, by embedding metallic magnetic nanoparticles into an appropriate insulating matrix and controlling their volume fraction and the particle sizes, it is possible to prepare an artificial electromagnetic medium which is left-handed for electromagnetic waves propagating in a frequency region near the resonance frequency [28]. Negative permeability can be obtained by resonance-type instead of relaxation-type frequency dispersion of permeability, whereas metallic materials do have negative permittivity below the plasmon frequency [29]. The potential of Fe@Al_2O_3 nanoembedments is therefore high.

4. Conclusions

In conclusion, Fe@Al_2O_3 nanoembedments were prepared from the mixture of magnetite and aluminum by mechanosynthesis. The magnetic measurement seems to be a suitable method to trace the microstructural evolution, since coercivity is microstructure sensitive. The overall milling process could be divided into two stages. In the first stage, the reaction in the Al-Fe_3O_4 mixture, a ductile–brittle system, is a highly exothermic one. The reactant mixture is continuously refined until the mechanochemical reaction is triggered. In the resulting alumina matrix, the embedded Fe nanoparticles have a wide size distribution from several nanometers to tens nanometers. In the second stage, Fe-Al_2O_3, another ductile–brittle system but chemically stable, is involved. The main microstructural change is the size and its distribution of iron nanoparticles. Extensively milling seems to significantly narrow the size distribution of Fe particle and increase the average particle size. Interestingly, the microwave permeability spectra exhibit a multiresonance behavior, which is related to the fine iron nanoparticles of narrow size distribution. The result is in good agreement with the exchange resonance mode. The mechanosynthesized Fe@Al_2O_3 nanoembedments could be used as microwave absorption materials. For the microwave of different frequency, the resonance frequency of nanoembedments can be tuned through the control of the size of magnetic nanoparticles.

Acknowledgements

The authors acknowledge the supports of National Natural Science Foundation of China (50772061), Program for New Century Excellent Talents in University (NCET-10-518) and Provincial Science and Technology Development Project of Shandong (2007GG10003007, 2007BS04032).

References

[1] P. Tartaj, T. González-Carreño, O. Bomatí-Miguel, C.J. Serna, Phys. Rev. B 69 (2007) 094401.
[2] S. Savoie, T.W. Napporn, B. Morel, M. Meunier, R. Roberge, J. Power Sources 196 (2011) 3713–3721.
[3] E. Thirumal, D. Prabhu, K. Chattopadhyay, V. Ravichandran, J. Alloys Compd. 502 (2010) 169–175.
[4] R. Walia, J.C. Pivin, A.K. Chawla, R. Jayaganthan, R. Chandra, J. Alloys Compd. 509 (2010) L103–L108.
[5] M. Murali, Yallapu, F. Shadi, Othman, T. Evan, Curtis, K. Brij, Gupta, Meena Jaggi, C. Subhash, Chauhan, Biomaterials 32 (2011) 1890–1905.
[6] R.Y. Hong, H.P. Fu, G.Q. Di, Y. Zheng, D.G. Wei, Mater. Chem. Phys. 108 (2008) 132–141.
[7] X.G. Lu, G.Y. Liang, Q.J. Sun, C.H. Yang, J. Alloys Compd. (2011), doi:10.1016/j.jallcom.2011.01.101.
[8] A.H. Taghvaei, H. Shokrollahi, M. Ghaffari, K. Janghorban, J. Phys. Chem. Solids 71 (2010) 7–11.
[9] L.Y. Chen, Z.X. Xu, H. Dai, S.T. Zhang, J. Alloys Compd. 497 (2010) 221–227.
[10] S. Linderoth, M.S. Pedersen, J. Appl. Phys. 75 (1994) 5867–5869.
[11] S. Lee, J.M. Kim, H.S. Hong, S.K. Woo, J. Alloys Compd. 467 (2009) 614–621.
[12] V.G. de Resende, F.L. Garcia, A. Peigney, E. De Grave, Laurent.F Ch., J. Alloys Compd. 471 (2009) 204–210.
[13] S. Figueroa, J. Desimoni, P.C. Rivas, M.C. Caracoche, O.D. Sanctis, J. Am. Ceram. Soc. 89 (2006) 3759–3764.
[14] C. Suryanarayana, Prog. Mater. Sci. 46 (2001) 1–184.
[15] J.D. Bobić, M.M. Vijatović, S. Greičius, J. Banys, B.D. Stojanović, J. Alloys Compd. 499 (2010) 221–226.
[16] Gh.R. Amiri, M.H. Yousefi, M.R. Abolhassani, S. Manouchehri, M.H. Keshavarz, S. Fatahian, J. Magn. Magn. Mater. 323 (2011) 730–734.
[17] A.A. Cristóbal, P.M. Botta, P.G. Bercoff, E.F. Aglietti, H.R. Bertorello, J.M. Porto López, J. Alloys Compd. 495 (2010) 516–519.
[18] S. Sabooni, T. Mousavi, F. Karimzadeh, J. Alloys Compd. 497 (2010) 95–99.
[19] A.K. Sun, D.Z. Wang, Z.Z. Wu, Q.J. Cheng, J. Alloys Compd. 509 (2011) L74–L77.
[20] X. Ni, J. Ma, J. Li, D. Jiao, J. Huang, X. Zhang, J. Alloys Compd. 468 (2009) 386–391.
[21] P.M. Botta, R.C. Mercader, E.F. Aglietti, J.M. Porto LÓpez, Scripta Mater. 48 (2003) 1093–1098.
[22] J.F. Löffler, J.P. Meier, B. Doudin, J. Ansermet, W. Wagner, Phys. Rev. B 57 (1998) 2915–2924.
[23] C. Kittle, Phys. Rev. 73 (1948) 155–161.
[24] D.L. Leslie-Pelecky, R.D. Rieke, Chem. Mater. 8 (1996) 1770–1783.
[25] G. Viau, F. Fiévet-Vincent, F. Fiévet, P. Toneguzzo, F. Ravel, O. Acher, J. Appl. Phys. 81 (1997) 2749–2754.
[26] A. Aharoni, J. Appl. Phys. 81 (1997) 830–833.
[27] C. Binns, M.J. Maher, Q.A. Pankhurst, D. Kechrakos, K.N. Trohidou, Phys. Rev. B 66 (2002) 184413.
[28] S.T. Chui, L.B. Hu, Phys. Rev. B 65 (2002) 144407.
[29] J.S. Wei, M.F. Xiao, J. Phys. Condens. Mater. 19 (2007) 072203.